This article was downloaded by:
On: *25 January 2011*
Access details: *Access Details: Free Access*
Publisher *Taylor & Francis*
Informa Ltd Registered in England and Wales Registered Number: 1072954 Registered office: Mortimer House, 37-41 Mortimer Street, London W1T 3JH, UK

Separation Science and Technology
Publication details, including instructions for authors and subscription information:
http://www.informaworld.com/smpp/title~content=t713708471

Adsorption Thermodynamic and Kinetic Studies of Fluoride Aqueous Solution Treated with Waste Iron Oxide

Chia-Chi Chang[ab]; Yao-Hui Huang[ab]; Hung-Ta Chen[ab]
[a] Department of Chemical Engineering, National Cheng Kung University, Tainan City, Taiwan [b] Sustainable Environment Research Center, National Cheng Kung University, Tainan City, Taiwan

Online publication date: 12 February 2010

To cite this Article Chang, Chia-Chi , Huang, Yao-Hui and Chen, Hung-Ta(2010) 'Adsorption Thermodynamic and Kinetic Studies of Fluoride Aqueous Solution Treated with Waste Iron Oxide', Separation Science and Technology, 45: 3, 370 — 379
To link to this Article: DOI: 10.1080/01496390903484826
URL: http://dx.doi.org/10.1080/01496390903484826

PLEASE SCROLL DOWN FOR ARTICLE

Full terms and conditions of use: http://www.informaworld.com/terms-and-conditions-of-access.pdf

This article may be used for research, teaching and private study purposes. Any substantial or systematic reproduction, re-distribution, re-selling, loan or sub-licensing, systematic supply or distribution in any form to anyone is expressly forbidden.

The publisher does not give any warranty express or implied or make any representation that the contents will be complete or accurate or up to date. The accuracy of any instructions, formulae and drug doses should be independently verified with primary sources. The publisher shall not be liable for any loss, actions, claims, proceedings, demand or costs or damages whatsoever or howsoever caused arising directly or indirectly in connection with or arising out of the use of this material.

Separation Science and Technology, 45: 370–379, 2010
Copyright © Taylor & Francis Group, LLC
ISSN: 0149-6395 print/1520-5754 online
DOI: 10.1080/01496390903484826

Taylor & Francis
Taylor & Francis Group

Adsorption Thermodynamic and Kinetic Studies of Fluoride Aqueous Solution Treated with Waste Iron Oxide

Chia-Chi Chang,[1,2] Yao-Hui Huang,[1,2] and Hung-Ta Chen[1,2]

[1]*Department of Chemical Engineering, National Cheng Kung University, Tainan City, Taiwan*
[2]*Sustainable Environment Research Center, National Cheng Kung University, Tainan City, Taiwan*

Downloaded At: 08:51 25 January 2011

This study uses a waste iron oxide material (BT3), which is a by-product of the fluidized-bed Fenton reaction (FBR–Fenton), for the treatment of a fluoride (F^-) solution. The purpose of this study is to investigate a low-cost sorbent as a replacement for the current costly methods of removing fluoride from wastewater. X-ray powder diffraction (XRD) and scanning electron microscopy (SEM) are used to characterize the BT3. Contact time, F^- concentration (from 0.75 to 6 mmol L^{-1}), and temperature (from 303 to 323 K) are used as operation parameters to treat the fluoride. The highest F^- adsorption capacity of the BT3 adsorbent was determined to be 1.17 mmol g^{-1} (22.2 mg g^{-1}) for a 6 mmol L^{-1} initial F^- concentration at pH 3.9 ± 0.2 and 303 ± 1 K. Adsorption data were well described by the Langmuir model, and the thermodynamic constants of the adsorption process, ΔG°, ΔH°, and ΔS°, were evaluated as -1.63 kJ mol^{-1} (at 303 K), -1.75 kJ mol^{-1}, and -52.4 J mol^{-1} K^{-1}, respectively. Additionally, a pseudo-second-order rate model was adopted to describe the kinetics of adsorption. BT3 could be regenerated with NaOH, and the regeneration efficiency reached 95.1% when the concentration of NaOH was 0.05 mol L^{-1}.

Keywords adsorption; fluoride; iron oxide

INTRODUCTION

Fluoride (F^-) is an essential component for the dental and bone health of mammals. However, excess fluoride in drinking water causes harmful effects such as problems relating to dental and skeletal fluorosis (1). The World Health Organization has set a guidance value of 1.5 mg L^{-1} for fluoride in drinking water (2), and the Taiwan drinking water standard for fluoride has been amended to 0.8 mg L^{-1}. Consequently, the treatment of fluoride has currently become an important subject worldwide. Fluoride waste can be found in the wastewater derived from industries such as those involved with semiconductors, metal processing, and the manufacture of fertilizer and glass (3). Many methods have been developed to remove excessive fluoride from water, including adsorption, ion exchange, precipitation, electrolysis, Donnan dialysis, and electrodialysis (4). Among these choices, precipitation is the most common and most economical of the methods used. In the precipitation method, chemicals such as lime ($Ca(OH)_2$), dolomite (magnesium salts), and alum ($Al_2(SO_4)_3$) have been widely used (5). Although the precipitation method is simple and economical, the required dosages are very high, which results in sludge disposal problems. Up to now, some treatment processes different from the classical methods referenced above, such as reverse osmosis, nanofiltration, electrodialysis, and Donnan dialysis, have been proposed in the literature on this topic. These processes also have some drawbacks (6–9). In order to overcome the inherent disadvantages, adsorption has been considered to be the most efficient and applicable technology for fluoride removal from waste water. In the past ten years, many researchers have devoted their attention to the development of low cost and effective adsorbent materials. A large number of materials have also been tested, such as alum sludge (10), activated alumina (11), amorphous alumina (12), metallurgical grade alumina (13), activated carbon (14), calcite (15), coal-based sorbent (16), fly ash (17), lanthanum impregnated silica gel (18), red mud (4) and some low cost adsorbents (19–21). However, they all have in common a low adsorption capacity (<10 mg/g) disadvantage. Therefore, more effective adsorbents in industrial fluoride wastewater treatment are required.

Recently, interest in low-cost, high-surface area materials, especially metal oxides, and their unique applications, such as adsorption and chemical catalysis, has been growing. Iron oxide has a relatively high surface area and charge; numerous researchers have used iron oxide as an adsorbent to treat heavy metals and anions from wastewater (22–26). This study elucidates an iron oxide adsorbent (BT3), which is a by-product resulting from the FBR–Fenton process (27,28), for use in treating wastewater from leather plants in Taiwan. This process not only provides a high COD removal efficiency but also reduces a large amount of the Fe sludge produced (27). However, the

Received 6 April 2009; accepted 29 October 2009.
Address correspondence to Yao-Hui Huang, Department of Chemical Engineering, National Cheng Kung University, Taiwan City, 701 Taiwan, Province of China. Tel.: +886 6 2757575 62636; Fax: +886 6 2344496. E-mail: yhhuang@mail.ncku.edu.tw

Downloaded At: 08:51 25 January 2011

iron oxide must be taken out of the FBR–Fenton reactor after an extended reaction. Therefore, the iron oxide-BT3 becomes a waste product. Hence, it is important to find another application for the waste iron oxide. In our previous studies, we successfully applied the iron oxide waste as an adsorbent for the removal of copper (Cu^{2+}) and lead (Pb^{2+}) from aqueous solutions (24,26). In this work, the tests and uses of a new iron oxide as an adsorbent for the removal of fluoride from aqueous solutions are carried out.

In this work, the removal of fluoride from aqueous solution using the BT3 is studied in batch experiments. The influences of time and pH on the adsorption capacity are investigated. We will examine the thermodynamics and kinetics of the adsorption of F^- by this BT3 adsorbent (i.e., iron oxide) to evaluate the thermodynamic parameters, to establish the adsorption rate equation, and to assess the effectiveness of iron oxide as an adsorbent of anions from wastewater. The experimental data were fitted to the Langmuir and Freundlich equations in order to determine which isotherm most closely correlates with the experimental data. The first-order Lagergren and second-order equations were adopted to fit the experimental data. Furthermore, the main object of this study is not only to reuse the by-product of the FBR–Fenton process but also to examine the feasibility and the superior capacity of BT3 in the adsorption of F^- as opposed to alternative adsorbents proposed in other studies.

MATERIAL AND METHODS

Materials

A novel and low cost adsorbent, iron oxide, was developed in the following manner (29): The iron oxide was packed as a carrier in a 25-m^3 (1.9 m-Φx 9 m-H) FBR-Fenton reactor in a wastewater treatment plant. By controlling the internal circulation, the superficial up flow velocity was maintained at 40 m/h with a 50% bed expansion. H_2O_2 (Union Chemical) and $FeSO_4$ (technical grade) with a molar ratio of 2:1 were fed into the reactor bottom continuously. The pH of the solution was controlled at 3.5 to prevent $Fe(OH)_3$ precipitation. The adsorbent, BT3, was a by-product of the FBR-Fenton reaction. The aqueous stock solution of sodium fluoride (NaF, Riedel-de Haen) was prepared using deionized water (Millipore Milli-Q).

Characterization of the Adsorbent

The physico-chemical characteristics of the BT3 adsorbent were elucidated using standard procedures. The Brunauer–Emmett–Teller (BET) surface area and porosity of the adsorbents were obtained from the isotherms. The surface area of the adsorbents was calculated from the BET equation. X-ray diffraction (XRD), Fourier transform infrared spectroscope (FTIR), and scanning electron microscopy (SEM) of the adsorbent were conducted. An XRD powder diffraction of the adsorbent was performed using a powder diffractometer (Rigaku RX III) with Cu K_α radiation. A small portion of BT3 was finely ground and then pressed (in a vacuum) in the form of a disc using spectroscopically pure dry KBr. The FTIR spectrum was recorded at room temperature using a Bio-Rad FTS-40A. The accelerating voltage and current were 40 kV and 20 mA, respectively. The morphology of the adsorbent was described using a Hitachi S-4100 SEM.

Batch Experimental Program

1 g of adsorbent was added to each of the various solutions with initial F^- concentrations from 0.75 to 6 mM (V = 1000 mL, pH 3.9 ± 0.2), in order to evaluate the thermodynamic properties. These samples were then mounted on the Jar Test apparatus continuously for 48 h at 303, 313, and 323 K. The pH of the solutions pH were controlled at 3.9 ± 0.2 by adding dilute HNO_3 or NaOH solutions during the entire experiment. The suspensions were filtered using a 0.45 μm syringe filter made of poly-(vinylidene fluoride) membrane, and the filtrates were immediately measured by ion-exclusion chromatography with a 4.6 mm ID × 250 mmL Metrosep A SUPP 1 column (Metrohm, USA). The amount adsorbed was determined as the difference between the initial and the equilibrium F^- concentrations. The kinetic of the adsorption experiment involved using the Jar Test at a constant speed of 100 revolutions per minute (rpm). The samples were prepared by adding 1 g of adsorbent to 1000 mL solution (pH = 3.9 ± 0.2); the F^- concentrations were 0.75, 1.5, 3 and 6 mmol L^{-1} at 303 ± 1 K. The amount of sorbed metal per gram of adsorbent q_t at time t was determined as follows (30):

$$q_t = \frac{C_0 - C_t}{m_{ads}}, \tag{1}$$

where C_0 is the initial F^- concentration of the liquid phase, and C_t is at any time t (in mg L^{-1}); m_{ads} is the amount of adsorbent in the solution (g L^{-1}). The pH of the solutions was adjusted with either HCl or NaOH solution.

Desorption experiments using NaOH were carried out. First fluoride was adsorbed according to the same procedure described above. Suspensions were centrifuged after adsorption. The supernatant was decanted and analyzed for fluoride. Then 1 L of NaOH solution (0.005∼0.2 M) were added to the loaded particles (1 g). The samples were stirred at 100 rpm at room temperature (30 ± 1°C) for 2 h. Then the samples were centrifuged and the supernatant was analyzed for fluoride. Regeneration efficiency was calculated.

Downloaded At: 08:51 25 January 2011

RESULTS AND DISCUSSION

Characterization of the Adsorbent

Figure 1 displays the two different magnifications of the morphology of the BT3 adsorbent shown as an oval shape with irregular surface morphology, which indicates high surface area. Table 1 presents the characteristics of the BT3 adsorbent. The average particle size is about 0.23 mm. Furthermore, the bulk density and absolute (true) density are 1.56 and 2.38 g cm^{-1}, respectively, which indicates that it is easy to separate adsorbents from aqueous solutions. The value of 105 m^2g^{-1} for the specific surface area also indicates that the BT3 adsorbent has a high surface area. Furthermore, the results also show a high value of total iron content (663 g kg^{-1}). A comparison of the BT3 adsorbent with the F1 (The average particle size is about 0.39 mm and total iron content is 304 g kg^{-1}) from our previous study (24) reveals that the BT3 adsorbent shows a smaller particle size and specific surface area but a higher total iron content than that of F1.

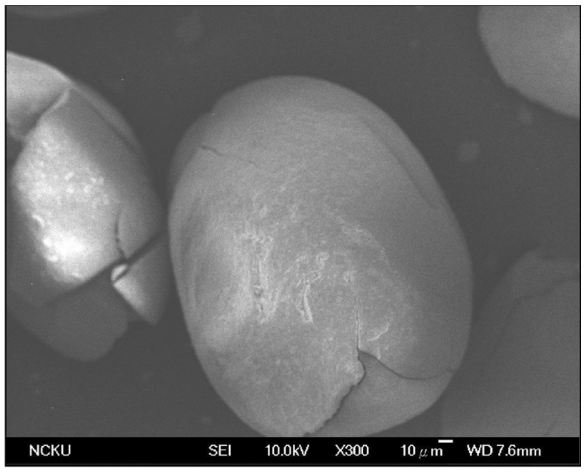

(a)

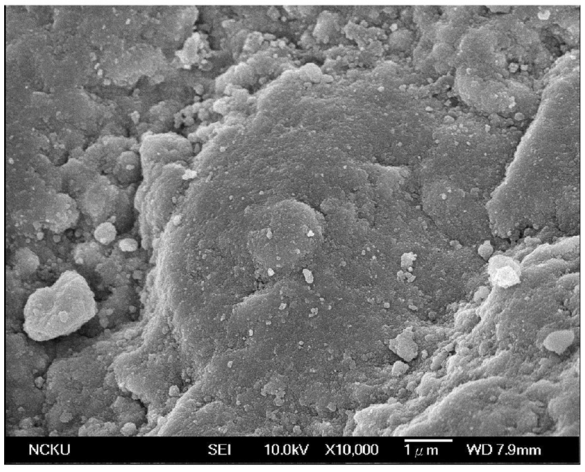

(b)

FIG. 1. Scanning electron micrographs of BT3: (a) 300 ×, (b) 10,000×.

TABLE 1
Properties of the BT3 adsorbent

Parameter	Value
Total iron content (g kg^{-1})	663
Bulk density (g cm^{-1})	1.56
Absolute (true) density (g cm^{-1})	2.38
Specific surface area ($m^2 g^{-1}$)	105
Total pore volume ($cm^3 g^{-1}$)	0.15
Average particle size (mm)	0.23

Figure 2 shows the XRD patterns of the BT3 adsorbent. The XRD data were analyzed from the BT3 adsorbent of iron according to the diffraction files of the Joint Committee on Powder Diffraction Standards (JCPDS). The JCPDS data on oxyhydroxides of iron were compared. The main diffraction peaks of the BT3 adsorbent at $2\theta = 21.2°$, 36.6°, and 53.2° were carefully compared with the standard for goethite (α-FeOOH—file number 81-0464). Accordingly, the peaks of BT3 adsorbent were identified with the phase α-FeOOH. However, the XRD pattern of the BT3 adsorbent exhibited very weak diffraction intensities in the region $2\theta = 10 \sim 80°$, indicating that the BT3 adsorbent contained a very small amount of crystalline goethite.

Figure 3 shows the FTIR spectrum of the BT3 adsorbent. It is clear that the peaks occur in the regions around 795, 883, 975, 1051, 1136, 1631, and 3169 cm^{-1}. When these peaks are eliminated from the analysis in the BT3 FTIR spectrum, only certain other significant peaks require identification. They show that the absorption band above 3000 wave number region is due to OH stretching

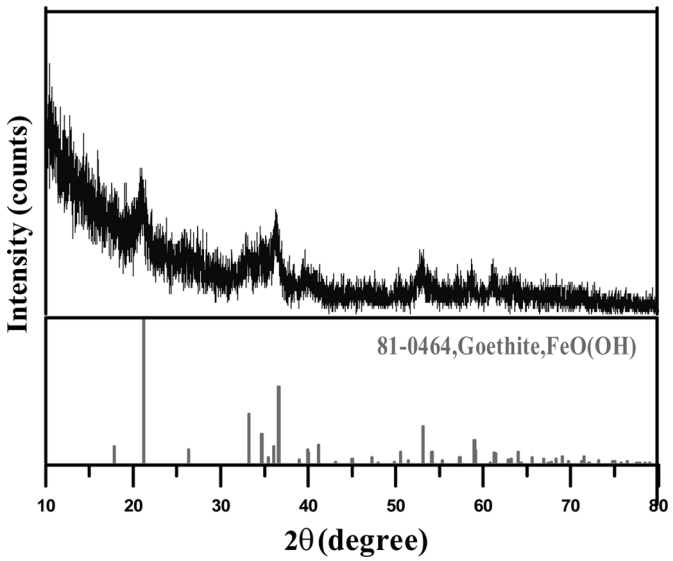

FIG. 2. X-ray diffraction pattern of BT3 showing the intensities in the region $2\theta = 10$–80°.

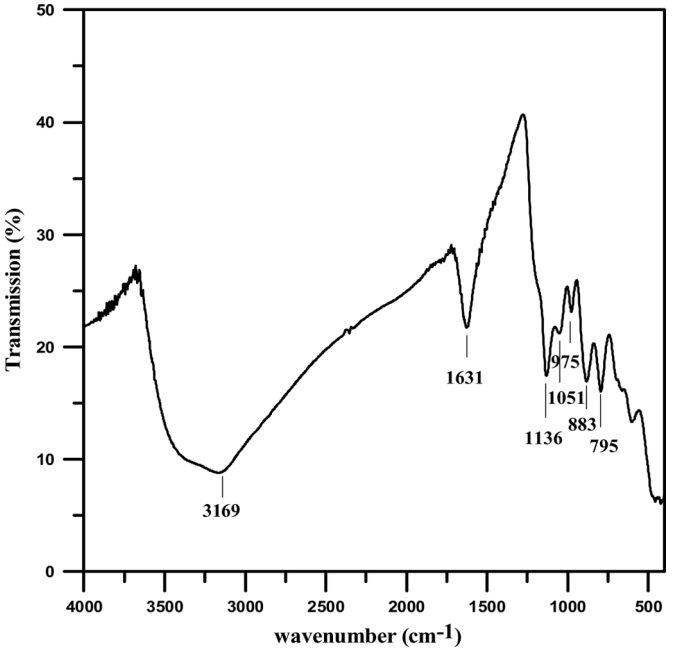

FIG. 3. FTIR spectrum from BT3.

Downloaded At: 08:51 25 January 2011

and that under 1000 wave number, this is due to Fe–O lattice vibration (31). The broad band seen at 3000–3500 cm^{-1} is due to hydration of the BT3. It is known that O–H stretching leads to a strong peak between 3000 and 3700 cm^{-1}, while the Fig. 3 FTIR spectrum from the BT3 indicates O–H bending to a medium band between 1200 and 1500 cm^{-1} (32,33). This result implies hydration in the BT3. Furthermore, it can be noted from Fig. 3 that the presence of α-FeOOH is confirmed by the appearance of peaks at 883 cm^{-1} (34) and 795 cm^{-1} (31). The pH value associated with a zero charge (pHzpc) on the BT3 adsorbent was around 4.1. More information on the method of measuring pHzpc is available elsewhere (35).

Effect of pH

The most important single factor that controls the adsorption of ions on the oxide surface is the pH of the aqueous solution. Since anion adsorption is coupled with a release of OH^- ion, so the adsorption of the fluoride on the BT3 surface is probably favoured in near neutral pH range (4).

The specific adsorption of fluoride on metal oxide is modeled as a two-step ligand-exchange reaction(36):

$$SOH + H^+ \longleftrightarrow SOH_2^+ \tag{2}$$

$$SOH_2^+ + F^- \longleftrightarrow SF + H_2O \tag{3}$$

which combined gives

$$SOH + H^+ + F^- \longleftrightarrow SF + H_2O \tag{4}$$

where S represents adsorbent. The adsorption of fluoride on BT3 was studied at different pH values ranging from 2 to 12. The adsorption of fluoride increases with increased pH, reaches a maximum of 20.4 mg/g at near pH 4 .0, and then decreases with further increase in pH (Fig. 4). The increased fluoride adsorption on BT3 at $pH < 4$ is due to the formation of weak hydrofluoric acid. However, the decreased fluoride adsorption on BT3 at $pH > 4$ is due to change of the surface nature of the oxide. At pH > pHzpc (4.10), the oxide surface becomes negative. The effect will help reduce sorption.

Adsorption Isotherm

Figure 5 shows the adsorption isotherms of F^- on BT3 at 303, 313 and 323 K, respectively. Equilibrium data can be analyzed using commonly known adsorption isotherms, which provide the basis for the design of adsorption systems. The most widely used isotherm equation for modeling of the adsorption data is the Langmuir equation, which is valid for monolayer sorption onto a surface with a finite number of identical sites and is given by Eq. (5).

$$q_e = \frac{K_L q_m C_e}{1 + K_L C_e}, \tag{5}$$

where K_L is the adsorption equilibrium constant including the affinity of the binding sites (mM^{-1}); q_m is the

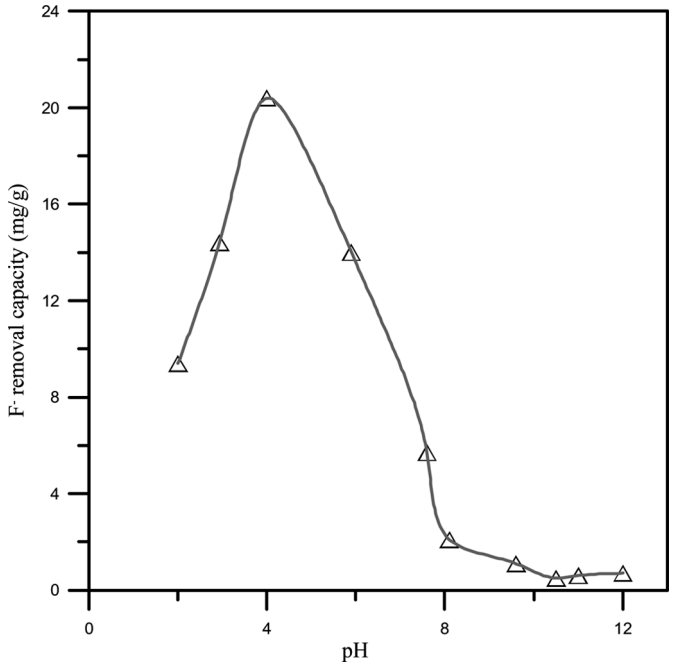

FIG. 4. Effect of pH on F^- removal using BT3 at 303 K with reaction conditions initial fluoride concentration 6 mmol L^{-1} and dosage 1 g L^{-1}.

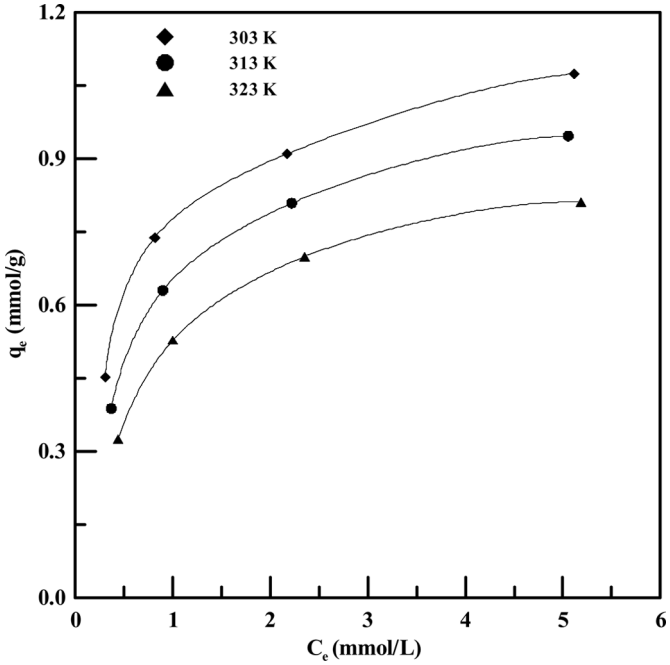

FIG. 5. Adsorption isotherms of F^- onto BT3 at different temperatures.

maximum adsorption capacity (mmol g^{-1}), and q_e is the amount of sorbed F^- at equilibrium (mmol g^{-1}). This represents a practical limiting adsorption capacity when the surface is fully covered with F^-. q_m and K_L can be determined from the linear plot of C_e/q_e versus C_e (37,38).

The Freundlich model is an empirical equation based on sorption on a heterogenous surface. It is given as:

$$q_e = K_F C_e^{1/n}, \tag{6}$$

where K_F and n are the Freundlich constants related to the adsorption capacity and adsorption intensity, respectively. The Freundlich equation can be linearized by taking logarithms, and constants can be determined (37).

The linear plots of C_e/q_e versus C_e and ln q_e versus ln C_e are shown in Figs. 6a and b. For each isotherm in Fig. 6a, the values of q_m and K_L were calculated from experimental data through linear regression. According to Fig. 6b, the values of K_F and n are obtained similarly. The results are presented in Table 2 with the correlation coefficients (R^2). It can be seen from Table 2 by comparing the results of the correlation coefficient values at different temperatures that the Langmuir model yields a better fit than the Freundlich. The values of Freundlich constants decreased with increasing temperature, and the highest K_F value was reported as 5.5 at 303 K. All n values were found to be high enough for adsorption (>1.0). Values of q_m and K_L at different temperatures are also tabulated in Table 2. The maximum capacity, q_m, defined the total capacity of BT3 for F^- adsorption and decreased with increasing temperature. Its maximum value was determined as 1.17 mmol g^{-1} (22.2 mg g^{-1}) at 303 K. The decrease of the sorption equilibrium constant with temperature showed that there was a chemical interaction between adsorbent and adsorbate. The fluoride adsorption performance of BT3 at room temperature has been assessed

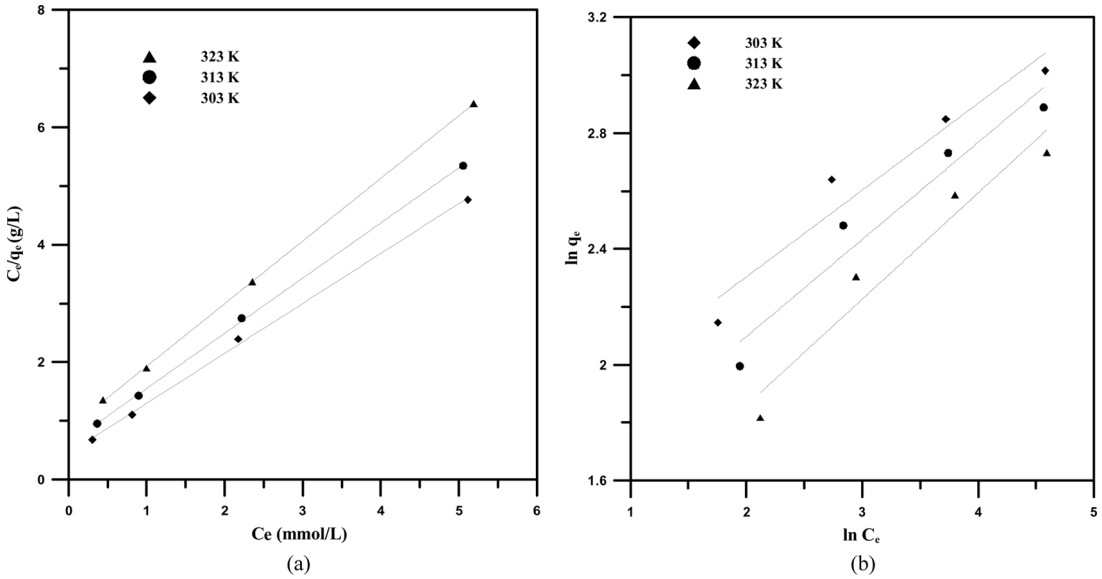

FIG. 6. Linearized: (a) Langmuir and (b) Freundlich isotherm models for F^- adsorption by BT3 at different temperatures.

Downloaded At: 08:51 25 January 2011

TABLE 2
Parameters of Langmuir and Freundlich adsorption isotherm models for F^- on BT3

	Langmuir			Freundlich		
T (K)	q_m	K_L	R^2	K_F	n	R^2
303	1.17	1.91	0.9988	5.50	3.34	0.9417
313	1.06	1.54	0.9997	4.14	2.98	0.9456
323	0.94	1.24	0.9999	3.08	2.72	0.9443

by comparing the monolayer adsorption capacity (q_m^*, mg g^{-1}) although the value is temperature dependent, as is supported by some of the available data from literature on this subject (Table 3) (39). The results obtained showed that BT3 has greater affinity for fluoride than has been indicated in earlier reported data.

Furthermore, entropy and energy factors should be considered in order to determine what processes will occur spontaneously in engineering practice. The Gibbs free energy indicates the degree of spontaneity of the adsorption process, and a higher negative value reflects a more energetically favorable adsorption. The Gibbs free energy change of adsorption is defined as:

$$\Delta G^0 = -RT \ln K_L, \tag{7}$$

where R is the universal gas constant (8.314 J mol^{-1} K^{-1}), and T is the absolute temperature in Kelvin (40). The equilibrium constant may be expressed in terms of the standard enthalpy change of adsorption (ΔH°) and the entropy change of adsorption (ΔS°) as a function of temperature. The relationship between the K_L and temperature is given by the van't Hoff equation:

$$\ln K_L = \frac{-\Delta H^0}{RT} + \frac{\Delta S^0}{R}. \tag{8}$$

ΔH° and ΔS° can be obtained from the slope and intercept of the plot of ln K_L versus 1/T (34). The equilibrium constants obtained from the Langmuir model at 303, 313, and 323 K were used to determine the Gibbs free energy changes. Table 4 shows the Gibbs free energy values for the adsorption process. The ΔH° and ΔS° were determined as $-1.75\,kJ\,mol^{-1}$ and $-52.4\,J\,mol^{-1}$ K^{-1} from Fig. 7, respectively. The negative standard enthalpy change of $-1.75\,kJ\,mol^{-1}$ obtained in this study indicates that the adsorption of F^- by the BT3 adsorbent is exothermic, a fact which is evidenced by the decrease in the adsorption of F^-

TABLE 3
A comparative assessment on fluoride adsorption performance of BT3 with some literature available data[39]

Adsorbent	q_m^*, mg g^{-1}	Reference
Metallurgical grade alumina	12.57	Pietrelli (2005)
Active alumina	7.08	Pietrelli (2005)
Alum sludge	5.394	Sujana et al. (1998)
Hydroxyapatite	4.54	Fan et al. (2003)
Fluorspar	1.79	Fan et al. (2003)
Activated quartz	1.16	Fan et al. (2003)
Calcite	0.39	Fan et al. (2003)
Quartz	0.19	Fan et al. (2003)
Activated alumina	2.41	Ghorai and Pant (2005)
Lignite	7.09	Sivasamy et al. (2001)
Bituminous coal	7.44	Sivasamy et al. (2001)
Iron-Zirconium Hybrid Oxide (IZHO)	8.21	Biswas et al. (2007)
Hydrous ferric oxide	7.50	Dey et al. (2004)
Hydrous zirconium oxide	10.21	Goswami et al. (2004)
Iron oxide (BT3)	22.2	Present work

q_m^*, value is compared taking the value obtained from the linear analysis of Langmuir model as other values shown are given from the analysis of same model.

Downloaded At: 08:51 25 January 2011

TABLE 4
ΔG° values for adsorption of F^- on BT3 at different temperatures

Temperature (K)	K_L (mM^{-1})	ΔG°(kJ/mol)
303	1.91	−1.63
313	1.54	−1.12
323	1.24	−0.59

with temperature. A negative change in adsorption standard free energy reveals that the adsorption reaction is a spontaneous process (40,41). The negative standard entropy change may have been caused by adsorption between the adsorbate and the BT3 adsorbent. These results were similar to those shown in previous literature (42) which indicated that although the standard enthalpy change for adsorption of very different adsorbate onto distinct adsorbent covers a wide range (−85 to +160 kJ mol^{-1}), the standard free energy change at 30°C remains within ±30 kJ mol^{-1}. Restated, the enthalpy and entropy contributions for driving the adsorption process largely compensate each other for very different adsorbate/adsorbent systems. This phenomenon needs further investigation since if it is correct, the reason why a universal correlation could exist between the corresponding enthalpy change and entropy change following adsorption remains unclear (42).

Kinetics of Adsorption

The adsorption kinetics that yield the solute uptake rate are the most important determinant of the adsorption efficiency of the BT3 adsorbent and therefore, its potential application. Figure 8 presents the effect of the contact time on the F^- adsorption rate for various concentrations. According to Fig. 8, the F^- adsorption rates increase dramatically during the first 24 h at various initial concentrations, reaching equilibrium slowly at 48 h. The first-order Lagergren Eq. (9), the pseudo-second-order rate Eq. (10), and the second-order rate Eq. (11) were evaluated from the experimental data to evaluate the rate of adsorption of F^- onto the BT3 adsorbent (43,44) and are shown as follows:

$$\log\frac{q_e - q_t}{q_e} = -\frac{k_L t}{2.3}, \tag{9}$$

$$\frac{t}{q_t} = \frac{1}{k' q_e^2} + \frac{t}{q_e}, \tag{10}$$

and

$$\frac{1}{q_e - q_t} = \frac{1}{q_e} + kt, \tag{11}$$

where k_L is the Lagergren rate constant of adsorption (h^{-1}); k' is the pseudo-second-order rate constant of adsorption (g mg^{-1} h^{-1}); k is the rate constant (g mg^{-1} h^{-1}), and q_e and q_t are the amounts of metal ion sorbed (mg g^{-1}) at equilibrium and at time t, respectively.

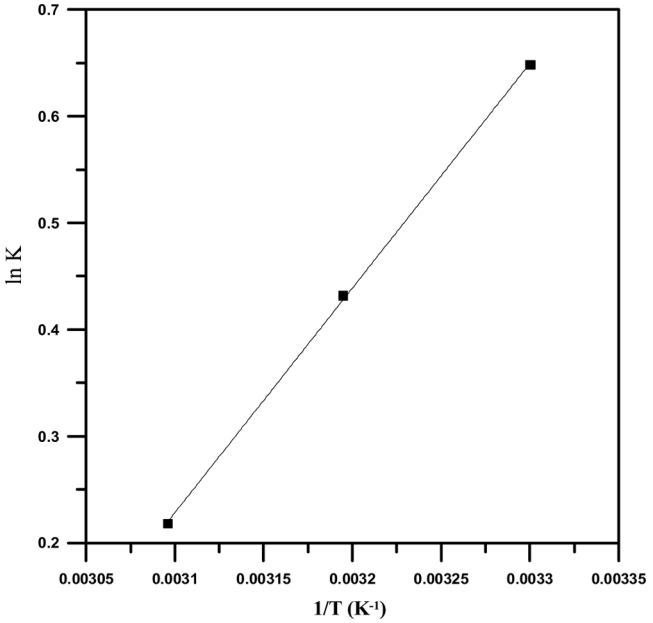

FIG. 7. ln K vs. 1/T plot.

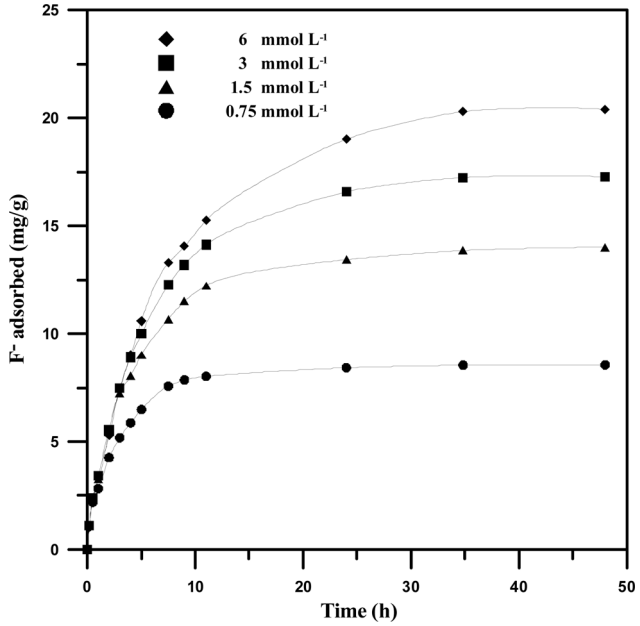

FIG. 8. Effect of contact time on F^- adsorption rate for different concentrations (pH 3.9 ± 0.2, at 303 ± 1 K).

Downloaded At: 08:51 25 January 2011

Figures 9a–c plots $\log(q_e - q_t)/q_e$ versus t, t/q_t versus t and $1/(q_e - q_t)$ versus t. These figures clearly indicate that the pseudo-second-order rate equation yields the best fit and that the correlation coefficients of the pseudo second-order rate model for the linear plots are very close to 1 at various concentrations (Fig. 9b), suggesting that kinetic adsorption can be described by the pseudo-second-order rate equation.

Desorption and Readsorption Capacity

To make a cost effective and user-friendly process, the adsorbent should regenerate, so as to reuse for further fluoride adsorption. The applicability of BT3 as a potential adsorbent depends on the desorption property and reusability also. NaOH solution was selected as the regeneration agent. The effect of NaOH concentration on desorption efficiency was plotted in Fig. 10. NaOH was efficient for

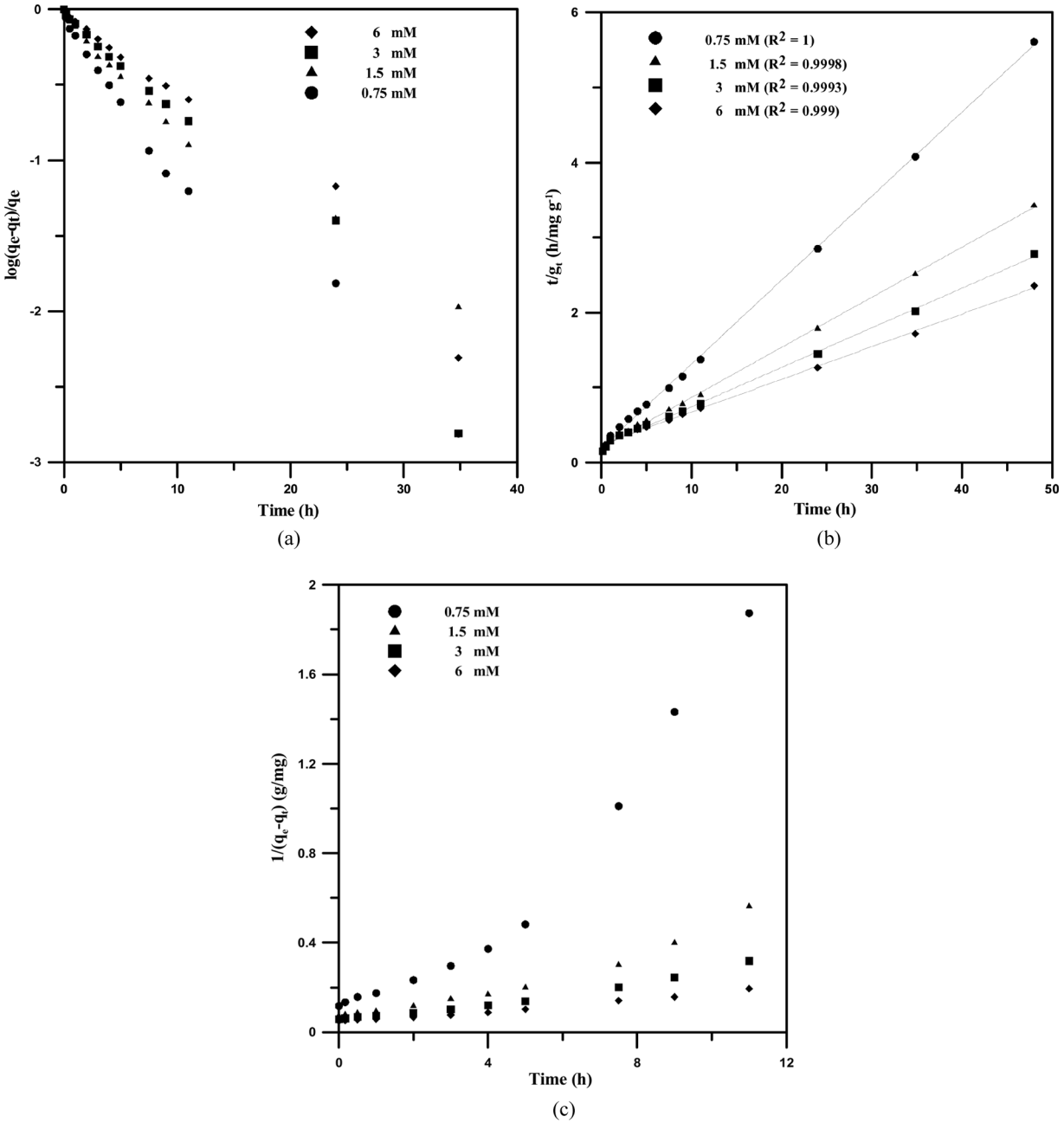

FIG. 9. Test of (a) the first-order Lagergren, (b) the pseudo-second-order and (c) the second-order rate equation for adsorption of different concentrations of F^- by BT3 adsorbent (pH 3.9 ± 0.2, at 303 ± 1 K).

Downloaded At: 08:51 25 January 2011

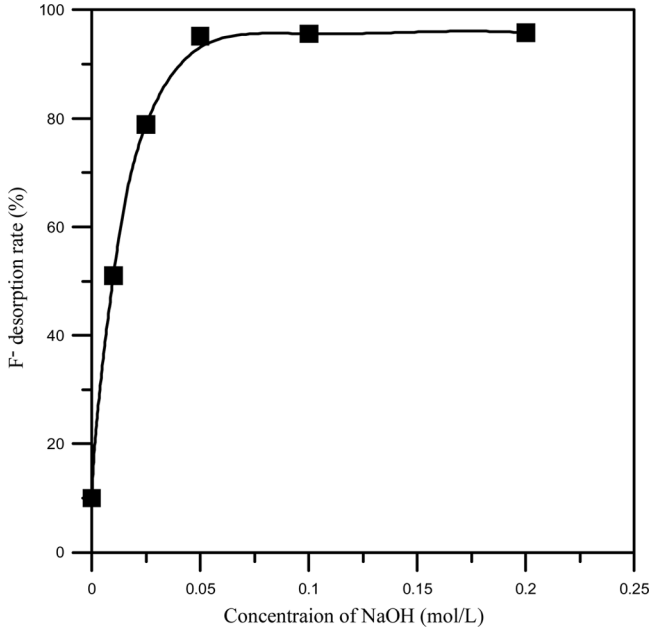

FIG. 10. Effect of NaOH concentration on desorption of fluoride.

BT3. The regeneration efficiency reached 79.9 and 95.1% when the concentration of NaOH reached 0.025 mol/L and 0.05 mol/L, respectively. A comparative experiment of BT3 and BT3 after regeneration was carried out. The effect of the dosage on F^- removal using BT3 and BT3 after regeneration was investigated. As seen from Fig. 11, the adsorption capacity of adsorbent after regeneration was equal to the BT3 untapped.

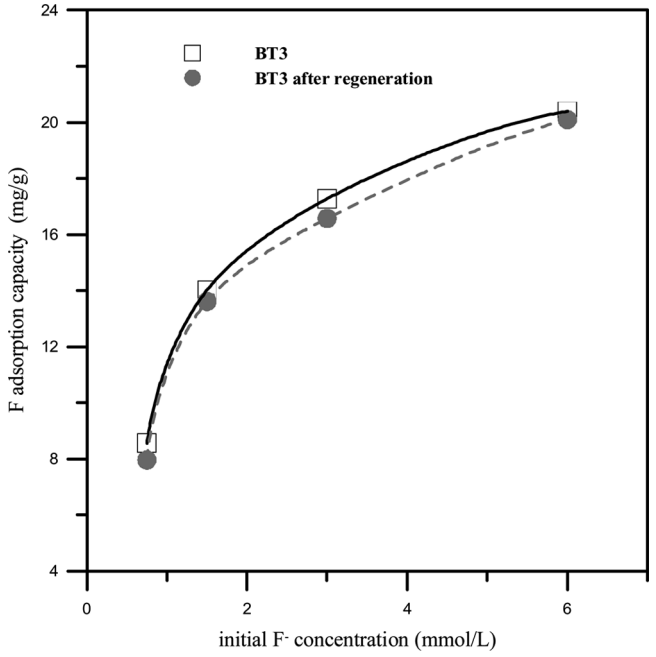

FIG. 11. Effect of the dosage on fluoride removal using BT3 and BT3 after regeneration at 303 K with reaction conditions pH 4.0, Initial fluoride concentration (mmol L^{-1}) used: 0.75, 1.5, 3, 6.

CONCLUSION

This work uses a new iron oxide as an adsorbent for the removal of fluoride from aqueous solutions. The ability of BT3 to bind of F^- was investigated with reference equilibrium, kinetics and thermodynamics. The maximum value of F^- adsorption capacity was determined to be 1.17 mmol g^{-1} (22.2 mg g^{-1}) at 303 K. The high adsorption capacity for fluoride suggests that BT3 can be used in industrial water treatment applications. The equilibrium data were well described by the Langmuir model. Furthermore, the negative standard enthalpy change suggests that the adsorption of F^- by the BT3 adsorbent is exothermic. The negative adsorption standard free energy changes reveal that the adsorption reaction is spontaneous. The pseudo-second-order rate model accurately describes the kinetics of adsorption. The optimum pH of removal of fluoride was found to be 4.0. The desorption efficiency of BT3 with NaOH reaches 95.1% when the concentration of NaOH is 0.05 mol/L. The adsorption capacity of the adsorbent after regeneration was equal to the BT3 untapped. The comparative study from Table 3 was successful in demonstrating the superior capacity of BT3 in the adsorption of F^- as compared to the adsorbents proposed in other studies, indicating a powerful potential for industrial application.

REFERENCES

1. Abe, I.; Iwasaki, S.; Tokimoto, T.; Kawasaki, N.; Nakamura, T.; Tanada, S. (2004) Adsorption of fluoride ions onto carbonaceous materials. *J. Colloid Interf. Sci.*, 275 (1): 35–39.
2. WHO. (2006) Chemical Fact Sheets: Fluoride. In: *Guidelines for Drinking Water Quality (Electronic resource): Incorporation First Addendum*, 3rd Ed.; Recommendations: Geneva; Vol. 1, 375–377.
3. Shen, F.; Chen, X.; Gao, P.; Chen, G. (2003) Electrochemical removal of fluoride ions from industrial wastewater. *Chem. Eng. Sci.*, 58 (3–6): 987–993.
4. Cengeloglu, Y.; Kir, E.; Ersoz, M. (2002) Removal of fluoride from aqueous solution by using red mud. *Sep. Purif. Technol.*, 28 (1): 81–86.
5. Yang, C.-L.; Dluhy, R. (2002) Electrochemical generation of aluminum sorbent for fluoride adsorption. *J. Hazard. Mater.*, 94 (3): 239–252.
6. Hichour, M.; Persin, F.; Sandeaux, J.; Gavach, C. (2000) Fluoride removal from waters by Donnan dialysis. *Sep. Purif. Technol.*, 18 (1): 1–11.
7. Amor, Z.; Bariou, B.; Mameri, N.; Taky, M.; Nicolas, S.; Elmidaoui, A. (2001) Fluoride removal from brackish water by electrodialysis. *Desalination*, 133 (3): 215–223.
8. Garmes, H.; Persin, F.; Sandeaux, J.; Pourcelly, G.; Mountadar, M. (2002) Defluoridation of groundwater by a hybrid process combining adsorption and Donnan dialysis. *Desalination*, 145 (1–3): 287–291.
9. Mjengera, H.; Mkongo, G. (2003) Appropriate deflouridation technology for use in flourotic areas in Tanzania. *Phys. Chem. Earth*, 28 (20–27): 1097–1104.
10. Sujana, M.G.; Thakur, R.S.; Rao, S.B. (1998) Removal of fluoride from aqueous solution by using alum sludge. *J. Colloid Interf. Sci.*, 206 (1): 94.

Downloaded At: 08:51 25 January 2011

11. Ghorai, S.; Pant, K.K. (2005) Equilibrium, kinetics and breakthrough studies for adsorption of fluoride on activated alumina. *Sep. Purif. Technol.*, 42 (3): 265–271.
12. Li, Y.H.; Wang, S.; Cao, A.; Zhao, D.; Zhang, X.; Xu, C., Luan, Z.R.D.; Liang, J.; Wu, D.; Wei, B. (2001) Adsorption of fluoride from water by amorphous alumina supported on carbon nanotube. *Chem. Phys. Lett.*, 350: 412–416.
13. Pietrelli, L. (2005) Fluoride wastewater treatment by adsorption onto Metallurgical grade alumina. *Ann. Chim.*, 95 (5): 303–312.
14. Srimurali, M.; Pragathi, A.; Karthikeyan, J. (1998) Study on removal of fluorides from drinking water by adsorption onto low-cost materials. *Environ. Pollut.*, 99 (2): 285–289.
15. Yang, M.; Hashimoto, T.; Hoshi, N.; Myoga, H. (1999) Fluoride removal in a fixed bed packed with granular calcite. *Water Res.*, 33 (16): 3395–3402.
16. Sivasamy, A.; Singh, K.P.; Mohan, D.; Maruthamuthu, M. (2001) Studies on defluoridation of water by coal-based sorbents. *J. Chem. Technol. Biot.*, 76 (7): 717–722.
17. Piekos, R.; Paslawaska, S. (1999) Fluoride uptake characteristics of fly ash. *Fluoride*, 32: 14–19.
18. Wasay, S.A.; Haron, M.J.; Tokunaga, S. (1996) Adsorption of fluoride, phosphate, and arsenate ions on lanthanum-impregnated silica gel. *Water Environ. Res.*, 68 (3): 295–300.
19. Fan, X.; Parker, D.J.; Smith, M.D. (2003) Adsorption kinetics of fluoride on low cost materials. *Water Res.*, 37 (20): 4929–4937.
20. Jamode, A.V.; Sapkal, V.S.; Jamode, V.S. (2004) Defluoridation of water using inexpensive adsorbents. *J. Indian I. Sci.*, 84 (5): 163–171.
21. Zhanga, J.; Xiea, S.; Hob, Y.-S. (2008) Removal of fluoride ions from aqueous solution using modified attapulgite as adsorbent. *J. Hazard. Mater.*, article in press.
22. Buamah, R.; Petrusevski, B.; Schippers, J.C. (2008) Adsorptive removal of manganese(II) from the aqueous phase using iron oxide coated sand. *J. Water Supply Res. T*, 57 (1): 1–11.
23. Gupta, V.K.; Saini, V.K.; Jain, N. (2005) Adsorption of As(III) from aqueous solutions by iron oxide-coated sand. *J.Colloid Interf. Sci.*, 288 (1): 55–60.
24. Huang, Y.-H.; Hsueh, C.-L.; Cheng, H.-P.; Su, L.-C.; Chen, C.-Y. (2007) Thermodynamics and kinetics of adsorption of Cu(II) onto waste iron oxide. *J. Hazard. Mater.*, 144 (1–2): 406–411.
25. Zeng, H.; Fisher, B.; Giammar, D.E. (2008) Individual and competitive adsorption of arsenate and phosphate to a high-surface-area iron oxide-based sorbent. *Environ. Sci. Technol.*, 42 (1): 147–152.
26. Huang, Y.-H.; Hsueh, C.-L.; Huang, C.-P.; Su, L.-C.; Chen, C.-Y. (2007) Adsorption thermodynamic and kinetic studies of Pb(II) removal from water onto a versatile Al_2O_3-supported iron oxide. *Sep. Purif. Technol.*, 55 (1): 23–29.
27. Chou, S.; Huang, C.; Huang, Y.-H. (1999) Effect of Fe^{2+} on catalytic oxidation in a fluidized bed reactor. *Chemosphere*, 39 (12): 1997–2006.
28. Chou, S.; Huang, C.; Huang, Y.-H. (2001) Heterogeneous and Homogeneous Catalytic Oxidation by Supported γ-FeOOH in a Fluidized-Bed Reactor: Kinetic Approach. *Environ. Sci. Technol.*, 35 (6): 1247–1251.
29. Huang; Yao-Hui (Hsinchu, TW), Huang; Gaw-Hao (Hsinchu, TW), Chou; Shan-Shan (Hsinchu, TW), You; Huey-Song (Hsinchu, TW), Perng; Shwu-Huey (Hsinchu, TW). (2000) Process for chemically oxidizing wastewater with reduced sludge production.
30. Chiron, N.; Guilet, R.; Deydier, E. (2003) Adsorption of Cu(II) and Pb(II) onto a grafted silica: Isotherms and kinetic models. *Water Res.*, 37 (13): 3079–3086.
31. Cornell, R.M.; Schwertmann, U. (2003) *The Iron Oxides*, 2nd Ed.; Wiley-VCH: New York.
32. Nyquist, R.A.; R.A.K. (Eds.) (1971) *IR Spectra of Inorganic Compounds*; Academic Press: New York.
33. Skoog, D.A.; Leary, J.J. (1992) *Principles of Instrumental Analysis*, 4th Ed.; Harcourt Brace College Publishers: New York; 252–309.
34. Misawa, T.; Asami, K.; Hashimoto, K.; Shimodaira, S. (1974) Mechanism of atmospheric rusting and the protective amorphous rust on low alloy steel. *Corrs. Sci.*, 14 (4): 279–289.
35. Stumm, W. (1992) *Chemistry of the Solid-Water Interface*; Wiley/Interscience: New York.
36. Tripathy, S.S.; Bersillon, J.-L.; Gopal, K. (2006) Removal of fluoride from drinking water by adsorption onto alum-impregnated activated alumina. *Sep. Purif. Technol.*, 50 (3): 310–317.
37. Smith, J.M. (1981) *Chemical Engineering Kinetics*, 3rd Ed.; McGraw-Hill: Singapore.
38. Langmuir, I. (1916) The constitution and fundamental properties of solids and liquids. *J. Am. Chem. Soc.*, 38: 2221–2295.
39. Biswas, K.; Bandhoyapadhyay, D.; Ghosh, U.C. (2007) Adsorption kinetics of fluoride on iron(III)-zirconium(IV) hybrid oxide. *Adsorption*, 13 (1): 83–94.
40. Smith, J.M.; Ness, H.C.V. (1987) *Introduction to Chemical Engineering Thermodynamics*, 4th Ed.; Mcgraw-Hill: Singapore.
41. Aksu, Z. (2002) Determination of the equilibrium, kinetic and thermodynamic parameters of the batch biosorption of nickel(II) ions onto Chlorella vulgaris. *Process Biochem.*, 38: 89–99.
42. Ramesh, A.; Lee, D.J.; Wong, J.W.C. (2005) Adsorption equilibrium of heavy metals and dyes from wastewater with low-cost adsorbents: A review. *J. Chin. Inst.Chem. Eng*, 203–222.
43. Benguella, B.; Benaissa, H. (2002) Cadmium removal from aqueous solutions by chitin: Kinetic and equilibrium studies. *Water Res.*, 36 (10): 2463–2474.
44. Ho, Y.-S. (2006) Review of second-order models for adsorption systems. *J. Hadard. Mater.*, 136 (3): 681–689.

Downloaded At: 08:51 25 January 2011